31st Congress of the International Council of the Aeronautical Sciences

Belo Horizonte, Brazil; September 09-14, 2018

TURBULENCE MODEL CONDITIONING FOR VORTEX DOMINATED FLOWS BASED ON EXPERIMENTAL RESULTS

Matteo Moioli* , **Christian Breitsamter*** , **Kaare A. Sørensen****
***Institute of Aerodynamics and Fluid Mechanics, Technical University of Munich ,**
****Airbus Defence and Space**

Keywords: *Delta wing, Turbulence modeling, Vortex flow, Computational Fluid Dynamics*

Abstract

Focusing on vortex dominated flows, related to delta wings, Reynolds Averaged Navier-Stokes numerical simulation with eddy viscosity models is an appropriate tool with respect to the computational effort. Nevertheless, higher accuracy is required to improve the prediction of the vortex flow development and characteristics. More complex turbulence models like Reynolds Stress Models introduce stability issues and increase the computational costs, not always improving the flow solution; Detached Eddy Simulation and Large Eddy Simulation models are not always a viable option due to computational resources. The idea introduced is to enhance the Spalart-Allmaras one-equation eddy viscosity model with additional destruction terms, exclusively active in the vortex region, optimized with experimental data as reference. The vortex topology is adjusted by correcting the distribution of eddy viscosity. The level of improvement in data accuracy, the range of improvements for the considered test cases and the flexibility of the model variation are investigated to understand the potential of the approach.

Nomenclature

AoA	Angle of attack, deg
C_L	Lift coefficient
C_D	Drag coefficient
C_{My}	Pitching moment coefficient
C_P	Pressure coefficient
d	Distance, m
c_r	Root chord, m
M	Mach number
Re	Reynolds number
s	Wing span, m
$S, \tilde{S}$	Strain rate, $1/s$
u, v, w	Velocity components, m/s
U_∞	Free stream velocity, m/s
x, y, z	Cartesian coordinates, m
$\mathcal{H}$	Helicity, m/s^2
μ	Dynamic viscosity, $kg/(ms)$
ν	Kinematic viscosity, m^2/s
μ_T	Dynamic eddy viscosity, $kg/(ms)$
$\nu_T, \tilde{\nu}$	Kinematic eddy viscosity, m^2/s
ξ	Vortex identifier quantity
ω	Vorticity, $1/s$

Subscripts

bv	Vortex production terms
bvb	Vortex breakdown production term
bvh	Vortex helicity-based terms

1 Introduction

The numerical simulation of delta wing geometries has been intensively studied for many years due to its complexity and relevance. Reynolds-Averaged Navier-Stokes (RANS) equations and Eddy Viscosity Models (EVM) are considered proper tools for numerical solutions at small to moderate angles of attack. As the angle of attack increases and the vortex flow pattern further complicates, i.e. multiple vortices are shed, interact and merge, the accuracy is progressively reduced

due to the limitation of EVMs to predict fully separated flows with high vorticity. During the years many experimental studies have been performed about vortical flows around delta wings. A vortex is generated as the shear layer separates from the leading edge and rolls up to form a core of high vorticity and axial velocity. The axial velocity in the core can reach three times the value of the free flow velocity [1, 2]. In addition, the rotational core induces high velocities near the wing surface resulting in a vortex induced suction peak, enhancing the lift coefficient. Outwards of the main vortex, a secondary counter-rotating vortex separates. The vortex strength grows as the angle of attack increases or as the sweep angle is reduced. When the vortex is strong enough an instability phenomenon, called vortex breakdown, takes place over the wing [3, 4] and the flow field changes abruptly. A drastic reduction of the core axial and circumferential velocites results in a strong reduction of the suction peak of the wing surface pressure. The breakdown phenomenon is clearly intricate by its own nature and, additionally, it manifests itself in different forms, i.e. the spiral and the bubble type.

Accordingly, it is evincible how EVMs often are not able to properly predict the main vortex characteristics. First of all, the separation onset of the vortex is possibly misrepresented, having implications on the vortex development downstream [5, 6, 7]. However, even if a sharp leading-edge geometry implies that the separation takes place over the whole leading-edge extension, the solution of the vortex flow features often lack accuracy as well [5, 6, 7, 8]. The turbulence model usually provides excessive eddy viscosity production in the vortex, with implications on the unburst vortex size, type and velocities. Consequently, the suction peak and the pressure distribution differ from experiments. The secondary vortex is possibly stronger or weaker, shifted or not present [5] and hence affecting also the main vortex position and development. The breakdown is usually misrepresented by numerical solutions with regard to its position and strength and, consequently, the sorrounding flow and the post-breakdown region are also negatively affected. The correct prediction of the vortex breakdown requires particular attention as the aerodynamic coefficients of a delta wing are highly sensitive to it.

When a delta wing is investigated, reliable experimental data are necessary to validate the numerical method and, in particular, the turbulence model characteristics. Therefore, the overview of many years of research and applications suggests the idea to utilize a relatively narrow range of experimental data to optimize and calibrate a modification of an one-equation EVM to enhance the accuracy for a wider range of cases. This possibility is considered an interesting option to be investigated instead of choosing more complex turbulence models which may introduce instabilities, extensive computational costs without guaranteeing an accuracy enhancement [9]. As already mentioned, vortex dominated flows manifest discrepancies due to a misprediction of the eddy viscosity destruction in the vortex flow. For this reason, the turbulence model modification is composed of additional eddy viscosity destruction terms which affect exclusively the vortex flow region. In order to extend the flexibility of the model enhancement, several terms are formulated with the aim of having different effects on different topologies and zones of a leading-edge vortex. The first phase of the research consists in investigating the different terms in their influences on the vortex flow solution for basic test cases. Consequently, a gradient-based optimizer is implemented in order to calibrate automatically the selected set of terms for a test case with experimental data as reference. Afterwards, the accuracy improvement provided by the optimized model and the dependence of the improvement on flow conditions and geometric variations are investigated. For this paper, two test cases are used: a 65° swept delta wing with interchangeable leading edges [10, 11] and a 76°/40° swept double delta wing with different fillet junction geometries [12].

2 Turbulence Model Enhancement

2.1 Spalart Allmaras Turbulence Model

The Spalart Allmaras (SA) one-equation Eddy Viscosity Model provides proper numerical solutions for wall-bounded flows [13]; nevertheless, the model manifests inaccuracies when large portions of separated flow or vortex dominated flows are considered. Vortex characteristics such as separation onset, strength and breakdown position can be misrepresented. Spalart and Shur [14] propose a streamline curvature correction (SA-RC) which adds to the production term a correction function. While the SA-RC modification can improve the accuracy for certain cases, it may also have a drastic impact on the vortex core and worsen the flow solution for other cases. It proves high dependence but low flexibility on the vortex characteristics and strength. The base turbulence model used here is the SA model with Edwards modification (SAE) [15].

$$\frac{D\tilde{\nu}}{Dt} = c_{b1}\tilde{S}\tilde{\nu} + \frac{1}{\sigma}\left[\nabla\cdot((\nu+\tilde{\nu})\nabla\tilde{\nu}) + c_{b2}(\nabla\tilde{\nu})^2\right] - c_{w1}f_w\left[\frac{\tilde{\nu}}{d}\right]^2 \quad (1)$$

With

$$c_{b1} = 0.1355 \qquad \sigma = \frac{2}{3} \qquad c_{b2} = 0.622 \quad (2)$$

$$c_{w1} = \frac{c_{b1}}{\kappa^2} + \frac{1+c_{b2}}{\sigma} \qquad \kappa = 0.41 \quad (3)$$

The proposed modification is composed of a set of additional destruction terms to be implemented in the SA equation. The near wall and the boundary layer solution have been a main goal during the original formulation and calibration of the SA model. For this reason and since the main focus of this research is the vortical flow solution, it has been chosen to isolate the effect of the additional terms on the vortical flow field and to mantain the original SA production term independent from the modification. Therefore, it mantains its calibration for the already validated attached flow and boundary layer solution.

2.2 Vortex Identification

A vortex identifier quantity is required to be coupled with additional terms in order to exclusively influence the vortex region. The SA-RC modification suggests the possibility to use the ratio between the strain rate S and vorticity ω as first idea for an identifier quantity.

$$r^* = \frac{S}{\omega} \quad (4)$$

The definition is correlated to the kinematic vorticity number N_k, defined by Truesdell [16]. N_k identifies a qualitative non-dimensional rotation region but returns no indication of the vorticity magnitude. Moreover, Jeong and Hussain [17] define a vortex as the region with $N_k > 1$.

$$N_k = \frac{\omega}{S} > 1 \quad (5)$$

At this point, it is possible and intuitive to define an appropriate quantity for the turbulence model variation, which is called ξ.

$$\xi = max\left[\left(\left(\frac{\omega}{S}\right) - c_{vl}\right), 0.0\right] \quad (6)$$

With

$$c_{vl} = 1 \quad (7)$$

Only positive values are provided by the vortex identifier quantity, the limitation of which is necessary because of the c_{vl} coefficient subtraction. The detraction coefficient c_{vl} has the objective to remove the influence of ξ from the boundary layer and, therefore, it is required to be calibrated through an investigation of the strain rate and vorticity ratio magnitude near the wall. As the only relevant component of the velocity gradient tensor in the boundary layer is $\frac{\partial u}{\partial z}$, the maximum value of the strain rate and vorticity ratio is equal to the value one and, therefore, the same value is associated with the detraction coefficient c_{vl}. The same value is also justified by the definition of Jeong and Hussain (5). The formulated quantity ξ is able to identify the vortex flow field and furthermore, to indicate its characteristics in terms of strength and stability by means of its distribution (Fig. 1). Therefore, it proves a proper

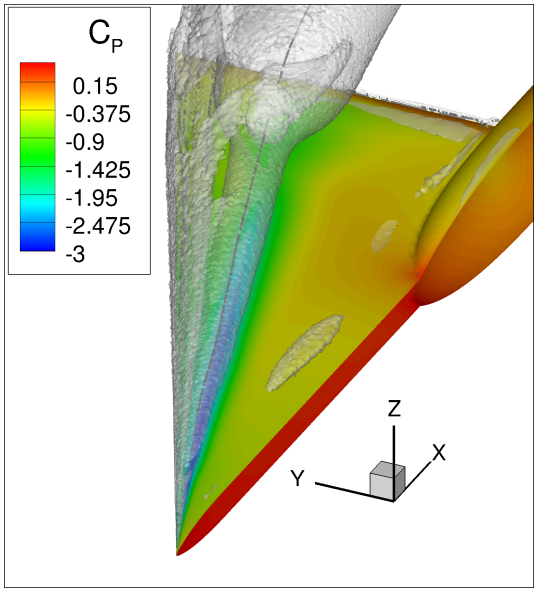

Fig. 1 Vortex flow identifier quantity ξ plotted as an iso-surface, $\xi = 0.1$, for the 65° delta wing test case at M = 0.4, Re = $6 \cdot 10^6$ and AoA = 20.4°; also shown: surface pressure coefficient distribution.

quantity on which base the terms formulation and to distinguish the effect over different types of vortices. It can be an important advantage when complicated flow fields are considered, e.g. multiple and interacting vortices.

2.3 Vortex Production Terms

The formulation of additional terms is based on the available knowledge about vortex flows and the investigation of the numerical solution for important test cases. Moreover, the terms are defined in order to have different effects and extend the flexibility of the approach to enhance various vortex topologies. After the phase of formulation, the set of terms is expanded, tested and improved with the aim to obtain a downselection to be used for successive applications.

The vortex terms, reported in Eq. (8), are formally consistent with the original term $c_{b1}\tilde{S}\tilde{\nu}$ in Eq. (1) and have the same physical dimension. The first term that is formulated is identified by the coefficient c_{bv1} and is similar to the original c_{b1} term but coupled with the vortex identifier quantity ξ. Additionally, two terms are formulated starting from c_{bv1} using a different exponentiation of the quantity ξ in order to have different influence regions in radial direction. The terms c_{bv2} and c_{bv3} (Fig. 2) have respectively a sublinear and superlinear dependence on ξ, i.e. an exponentiation of 0.5 and 2. While the c_{bv3} term concentrates on the vortex core, the c_{bv2} term becomes more flattened. Moreover, the influence on the outer part of the vortex is made stronger than the core effect by means of a negative exponentiation of ξ. An additional switch quantity ξ_{sw} based on the vortex identifier is necessary to ensure the influence of the c_{bv4} term is only present in the vortex flow field (Fig. 2).

$$\begin{aligned}\frac{D\tilde{\nu}}{Dt} &= c_{b1}\tilde{S}\tilde{\nu} - \Big[c_{bv1}\xi S\tilde{\nu} + c_{bv2}\xi^{\frac{1}{2}}S\tilde{\nu} + c_{bv3}\xi^2 S\tilde{\nu} \\ &+ c_{bv4}\left(min\left(\frac{1}{\xi}, c_{vr,lim}\right)\right)\xi_{sw}S\tilde{\nu} + c_{bvh1}\widetilde{\mathcal{H}}\xi\tilde{\nu} \\ &+ c_{bvh2}\left[max\left(min\left(\frac{1}{\widetilde{\mathcal{H}}}, 1.0\right), 0.0\right)\right]\xi\omega\tilde{\nu}\Big] \\ &+ c_{bvb}||\nabla V\frac{\omega}{||\omega||}||\xi\tilde{\nu} \\ &+ \frac{1}{\sigma}\left[\nabla\cdot((\nu+\tilde{\nu})\nabla\tilde{\nu}) + c_{b2}(\nabla\tilde{\nu})^2\right] - c_{w1}f_w\left[\frac{\tilde{\nu}}{d}\right]^2\end{aligned} \tag{8}$$

With

$$\mathcal{H} = V\cdot\omega \tag{9}$$

$$\widetilde{\mathcal{H}} = \frac{|\mathcal{H}|}{U_\infty} \tag{10}$$

Along the direction of the vortex core, the successive steps of the vortex evolution, i.e. the unburst vortex, the breakdown region and the post-breakdown flow, provide fundamental regions on which is to be distinguished the influence of further terms (Fig. 3). Being the unburst vortex characterized by a coherent structure with high values of axial and rotational velocity, the helicity $\mathcal{H}$ proves a proper quantity to identify the region and formulate a term c_{bvh1} accordingly. Firstly, the absolute value of $\mathcal{H}$ is evaluated to avoid dependence on the rotation direction and secondly the quantity is properly dimensionalized with the free stream velocity. The new

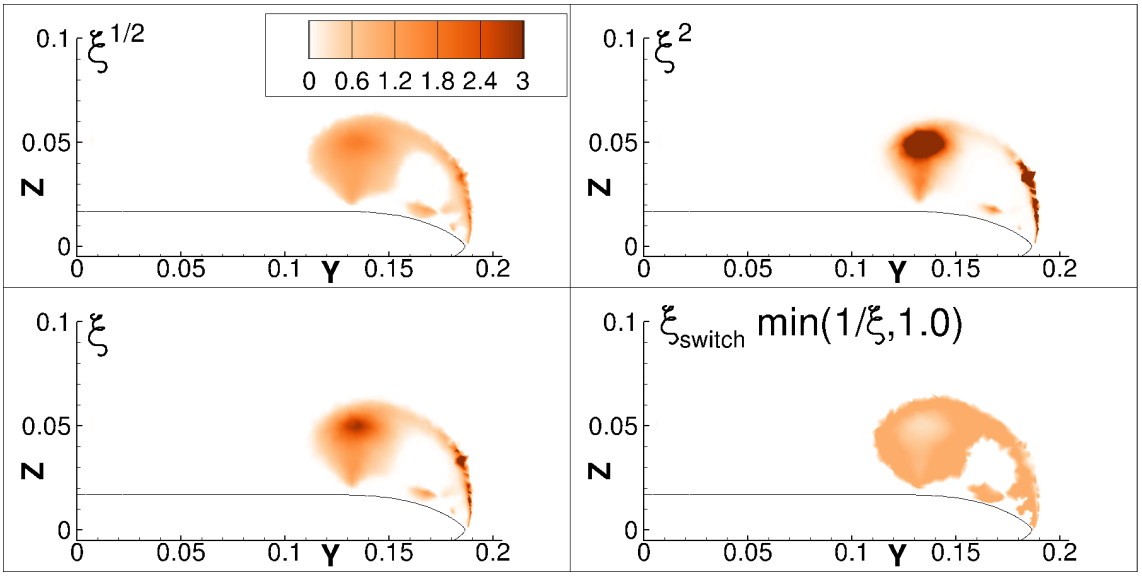

Fig. 2 Radial influence dependence on the exponentation of the vortex identifier quantity ξ shown for a cross flow plane at $x/c_r = 0.6$ for the 65° delta wing test case at M = 0.4, Re = $6 \cdot 10^6$ and AoA = 20.4°.

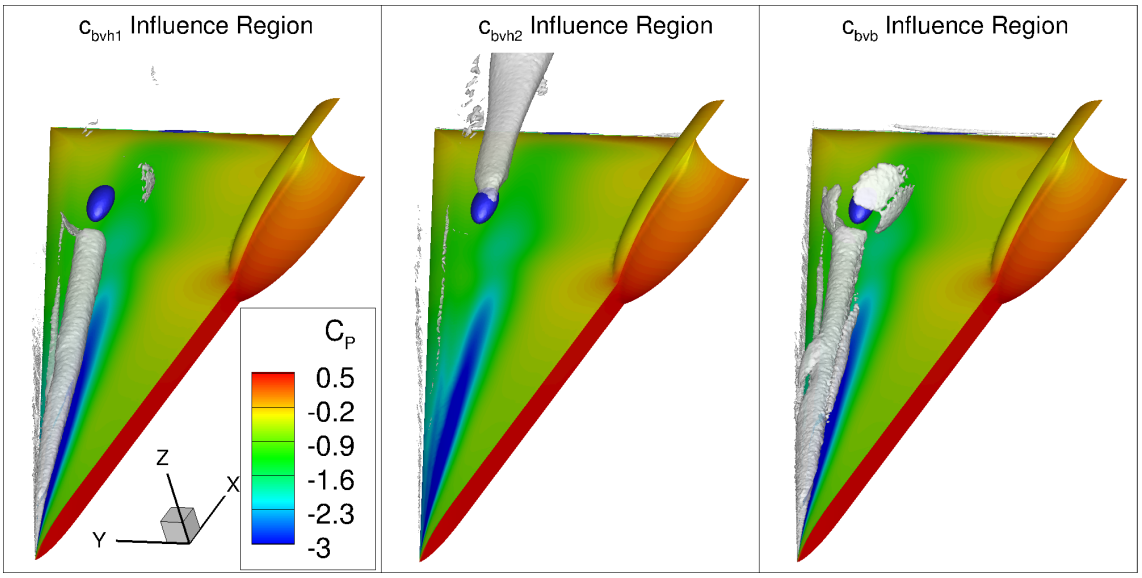

Fig. 3 Influence regions upstream, close and downstream of vortex bursting of the different terms c_{bvh1}, c_{bvh2} and c_{bvb} of the modified turbulence model for the 65° delta wing test case at M = 0.4 and AoA = 26.5°; also shown: surface pressure coefficient distribution.

quantity is identified as $\widetilde{\mathcal{H}}$. Downstream of the breakdown location, an incoherent and turbulent flow field is formed through the expansion of the vortex core and an abrupt reduction of axial and rotational velocities. Here the helicity quantity is almost negligible and, therefore, by formulating a switch quantity based on the reciprocal of $\widetilde{\mathcal{H}}$, the influence of a new term c_{bvh2} is concentraded on the post-breakdown region. At last, since the vortex breakdown is mainly characterized by large velocity gradients, considering the fact that axial and rotational velocities drop abruptly, a term c_{bvb}, which is dominant in the proximity of the breakdown, is formulated. Namely, the velocity gradient tensor is multiplied to the vorticity direction vector to obtain a vector, the norm of which

is dominant in the proximity of vortex breakdown. The formulated terms are analyzed by testing arbitrary coefficients on numerical computations and investigate their influence and the sensitivity of the solution to their values. In conclusion, with the information gathered, the terms are set to form the fulcrum of the turbulence model conditioning approach.

3 Results and Discussion

3.1 Test Cases and Optimization Procedure

The TAU-Code [18, 19], which is developed by DLR (German Aerospace Center), is used for the numerical simulation and the implementation of the turbulence model modifications. It uses a finite volume formulation and solves 3-D, compressible and steady or unsteady RANS equations on hybrid-unstructured grids. The solver settings are set up accordingly for the considered test cases and the computational grids are fixed following the investigation of different levels of fineness. The reported test cases are a 65° swept delta wing with interchangeable leading-edge geometries and a 76°/40° double delta geometry with different junction shapes. Initially, when a test case is selected, a subset of the experimental data available are chosen as objective of improvement and possible extensions to wider a spectrum of cases for the resultant optimized turbulence model are pre-estimated. Hence, preliminary investigations on the numerical solution with the original SAE model and a comparison with the wind tunnel experiments are performed. In accordance with the outcome of a first analysis of the main sources of error, the sensitivity and impact of the main additional terms are tested with single simulations in order to properly set up the automatic calibration procedure. Successively, the coefficients of the terms are adjusted by means of a gradient-based optimizer. It iteratively updates the coefficients of the additional terms for a base numerical simulation with the information of the error sensitivity to the terms variation, evaluated at the previous iteration. Eventually, it converges to an optimum of the average error between experimental data and the numerical simulation. The objective error is usually defined in terms of the average pressure coefficient error, but any relevant data from the wind tunnel experiments can be used. The optimum is often local, therefore different initial starting coefficients for the optimization are set in order to find better optima. For this purpose, the knowledge of the considered test case and prior experience of the approach give important insight. As a general approach, the optimization is firstly performed for a relevant angle of attack and, afterwards, the resultant calibration is applied, e.g. for the whole polar, in order to investigate the dependence on the angle of attack. In fact, since the vortex type and development is changing with the angle of attack, rotation correction approaches for the eddy viscosity field, for example SA-RC [14], can improve the results for the major part of the angle-of-attack polar while worsen for a smaller portion. In the case of the proposed approach, instead, having a minimum dependence on the angle of attack is an important condition for extending and improving its potential feasibility. It is expected that through the additional terms a higher control on the vortex solution can be acquired, reducing the dependency on angle of attack and moderate geometry variations. Therefore, when an optimized model is available, its accuracy improvement is investigated also for a wider range of flow conditions or geometric variations to understand the flexibility and globality of the optimized turbulence model variation.

3.2 Test Case: 65° Delta Wing

The 65° swept delta wing has been deeply studied from NASA [10] and in the context of the Second Vortex Flow Experiment (VFE-2) project [11]. Wind tunnel experiments have been performed for several flow conditions and leading-edge geometries. The wing geometry has been already used in the previous section to visualize the effect of the formulated terms (Fig. 1, 3). The subsonic regime, i.e. Mach number 0.4, Reynolds number of $6 \cdot 10^6$ and the small radius leading-edge

(0.05% of the mean aerodynamic chord) case is firstly investigated. For the considered leading-edge geometry, the vortex separation is present along the whole leading-edge extension, i.e. a fully developed leading-edge vortex is present, and this is in agreement with experiments. Therefore, the turbulence model conditioning can concentrate on the vortex solution in terms of vortex strength and breakdown position. For the standard SAE model solution at AoA = 20.4° (Fig. 4), the breakdown takes place over the wing, i.e. around 80% of the c_r, while the experiments show no breakdown at 95% of the c_r. By comparing the C_P distribution between SAE standard model results and experimental data for angles of attack of 16.3°, 20.4° and 26.5° (Fig. 5), the numerical solution shows a weaker suction peak in the front part, a premature breakdown position and, as consequence, discrepancies in the suction distribution on the rear half of the wing.

The optimization procedure is firstly performed on a single point of the polar (AoA = 20.4°) returning a 56% reduction of the average C_P error, i.e. from 0.153 to 0.067. Negligible

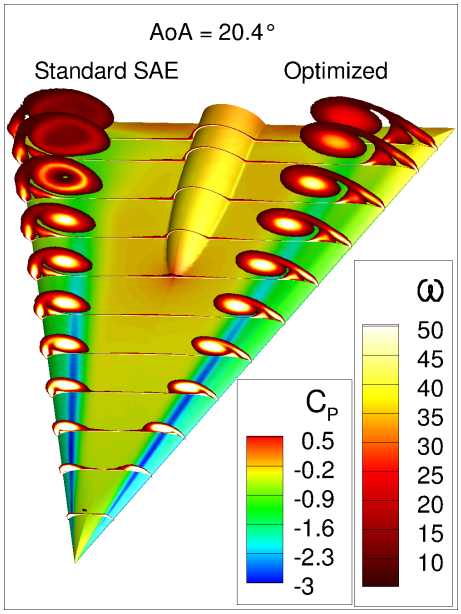

Fig. 4 Surface C_P distribution and vorticity magnitude in the vortex flow field, comparison between standard SAE and optimized model for the 65° delta wing, M = 0.4, Re = $6 \cdot 10^6$ and AoA of 20.4°.

dependence of the improvement on the angle of attack is given by similar optimizations on two points of the polar and from the application of the optimum on the whole polar, for which the error reduction consists of a 40%. The potential of the approach finds a first important confirmation in the manifested low dependence on the angle of attack, which suggests the capability of the variation to capture and enhance physical characteristics of the vortex development.

The C_P distribution (Fig. 5) shows clearly how the accuracy is improved along the whole polar. The major contribution to the error remains in the front part of the wing, where the solution has low sensitivity to the turbulence model. The breakdown position is delayed by the eddy viscosity variation, the high core vorticity is conserved longer (Fig. 4) and, therefore, the pressure peak is narrower and stronger. Moreover, the region outwards the vortex is improved even if the secondary vortex peak is often stronger than found in the experiments, where a definite suction peak is not present. The pressure side of the wing have zero sensitivity to the vortex turbulence model as expected, except for the pressure distribution near the trailing edge. With regard to the results obtained with the SA-RC model, they show an example of possible limitation of such an approach. On the one hand, at low angles of attack, the variation is comparable to the optimized model even if the effect is excessive. On the other hand, the vortex breakdown is moved upstream drastically and the influence acts in an opposite direction compared to the optimized model.

The globality of the optimized model is investigated by its application to available geometrical variations, i.e. sharp and medium radius leading-edges. The vortex structure changes partially, therefore a significant part of the improvement is conserved. As conclusion, it is shown how the approach provides improvments for a range of flow conditions and geometric variations by optimizing the turbulence model coefficients for a minor number of cases.

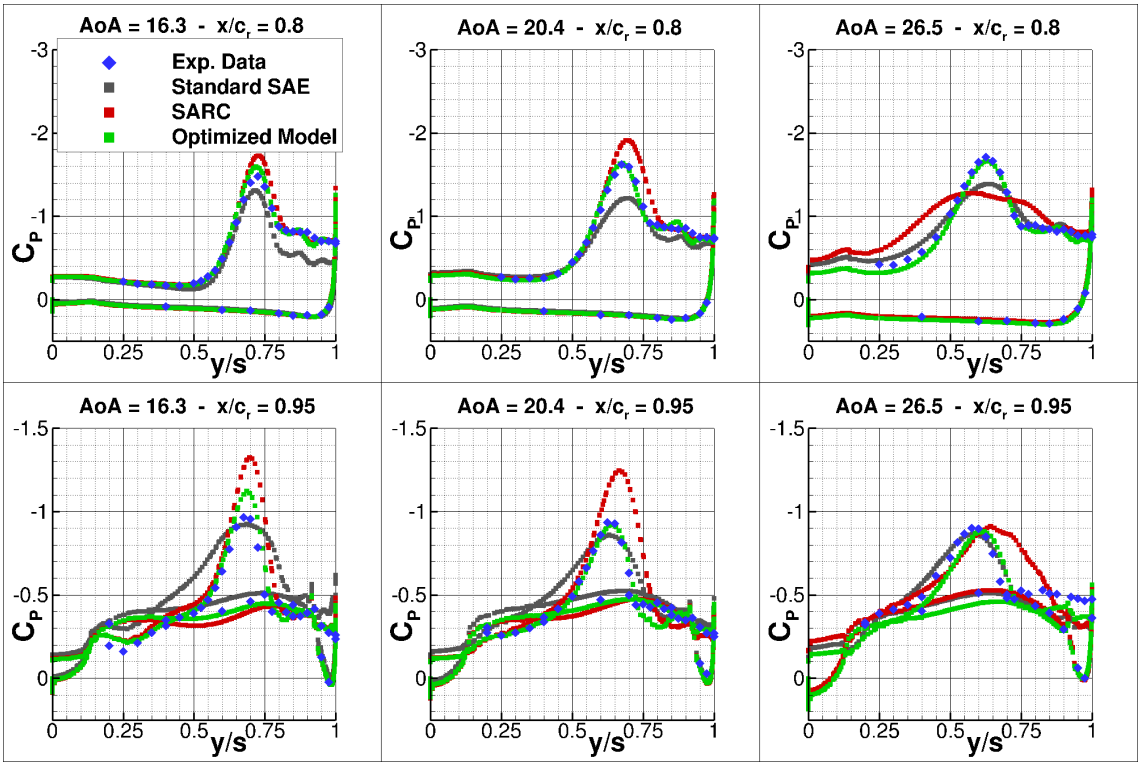

Fig. 5 Surface C_P distribution, comparison between experimental data [10], standard SAE, SA-RC and optimized model for the 65° delta wing with small radius leading-edge with M = 0.4, Re = $6 \cdot 10^6$ and AoA of 16.3°, 20.4° and 26.5°.

3.3 Double Delta Wing

In case of a double delta wing configuration, two vortices occur on the wing upper side and potentially differ in their topologies. They can introduce further sources of error in the EVM solution as they can interact and merge providing complex flow fields. The NASA double delta wing [12] provides a proper range of reliable experimental data for the research. The wing planform is composed by a strake of 76° sweep angle and a wing of 40° sweep angle. Three junction fillet variations are available. The highly swept strake generates a stable and strong vortex which energizes the second weaker vortex and delays the breakdown. The subsonic case at Mach number 0.5 is selected for the turbulence model optimization, including a portion of the angle-of-attack polar in the procedure. After a preliminary investigation of the terms sensitivity, the optimization is started from different set of terms and starting points in order to overcome the locality of the optium. Experimental data are available in terms of Pressure Sensitive Paint (PSP) images, static pressure measurements and integral forces; the integral forces are set as error objective for the optimizer.

3.3.1 Baseline Fillet

The large junction angle, i.e. the difference between strake and wing sweep angle, provokes a strong interaction between the vortices as the angle of attack increases. The main discrepancies between standard SAE model simulations and wind tunnel data are present at high angles of attack (Fig. 6), where the lift coefficient C_L is higher and suggests that the breakdown position is postponed in the numerical results. Consequently, lower values of the pitching moment coefficient C_{My} are provided and the pressure distribution comparison confirms how the high suction zone is maintained over the wing.

As the optimization procedure is started, during a first test phase, it is evincible how error re-

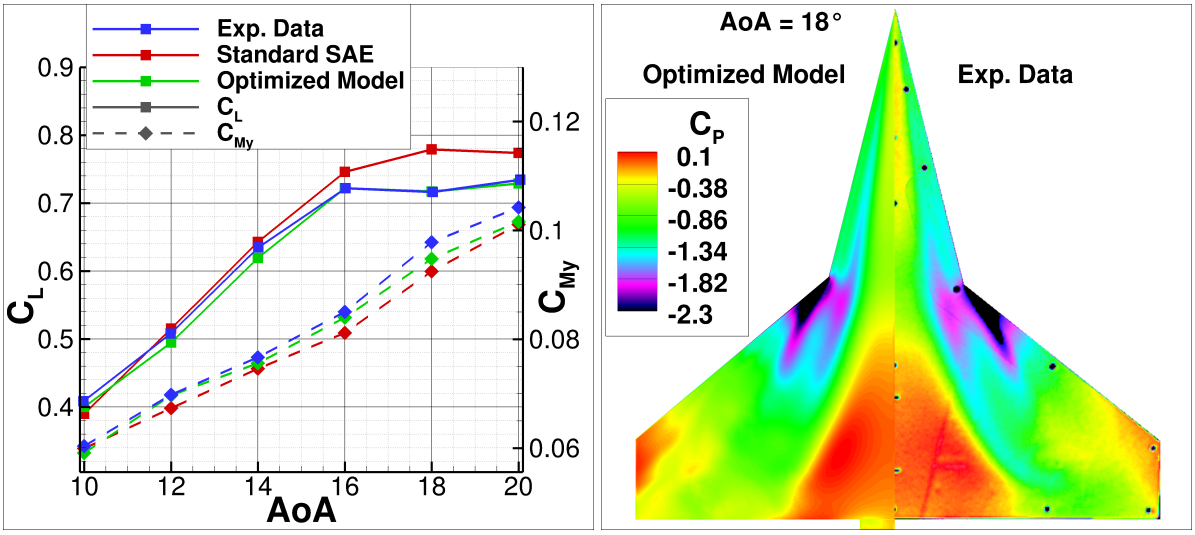

Fig. 6 Aerodynamic coefficients angle-of-attack polar and surface C_P for AoA = 18°, Comparison of experimental data [12], standard SAE and optimized model for the 76°/40° double delta wing with baseline fillet, M = 0.5, Re = $2 \cdot 10^6$.

duction is obtainable thanks to additional eddy viscosity destruction in the vortex. The direction of variation is consistent with the need to move upstream the breakdown over the wing. However, due to the fact that the two vortices may lead to different variations in the turbulence model coefficients, as consequence of their different topologies, the optimization is complicate. In addition, the wing vortex breakdown triggers the strake vortex breakdown adding cross-dependence between the turbulence model variations on the two vortical structures.

Even if the optimization is performed for a portion of the angle-of-attack polar, the error reduction for the integral forces consists of 44% on the whole polar. In fact, the polar (Fig. 6) is now closer to the experimental results and the most evident enhancement is in the C_L prediction for angles of attack higher than 14°, where the standard SAE model provides the biggest discrepancies. The optimized model improves the breakdown position compared to the experimental data (Fig. 6) and the C_{My} error also diminishes as the suction footprint is closer to the experiments. However the C_L variation is too strong for angles of attack of 12° and 14° even if the C_{My} is properly fitting the data. The sensitivity of the conditioned turbulence model on the angle of attack remains overall low which is a relevant quality for the potential of the approach. The strake vortex is less sensitive to the turbulence model variation. However, the variation is more relevant as the vortex approaches breakdown. A possibility to improve even further the optimized model would be to use the pressure distribution as objective for the optimization. In that case, a higher resolution of the measurements distribution over the wing would be favourable. The overall improvement is hence appreciable and promising.

3.3.2 *Parabolic Fillet*

The parabolic fillet has been designed, as reported by Erickson [12], with the aim to reduce the effect of the junction discontinuity and promote the formation of a single vortex over the wing. However, a smaller second vortex is visualized in the experiment and it separates due to the high junction angle. The weaker vortex rapidly merges into the stronger strake vortex. The vortex topology is drastically different compared to the baseline fillet and, therefore, it is reasonable to expect a different need in terms of turbulence model conditioning. In fact, the previously optimized model has low influence on the numerical solution of the parabolic fillet case and only slight differences from the standard

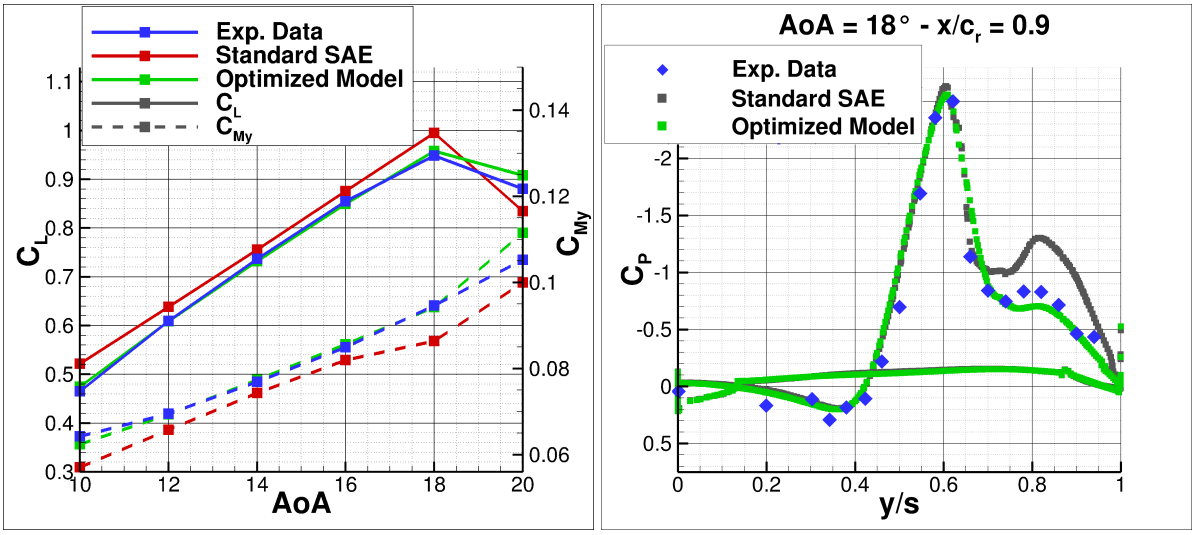

Fig. 7 Aerodynamic coefficients angle-of-attack polar and C_P distribution comparison for AoA = 18°, Comparison of experimental data [12], standard SAE and optimized model for the 76°/40° double delta wing with parabolic fillet, M = 0.5, Re = $2 \cdot 10^6$.

SAE model are evident. However, the standard SAE model manifests lack of accuracy along the angle-of-attack polar in terms of integral forces and in the pressure distribution (Fig. 7). An almost constant offset between experiments and numerical solutions is present with regard to both C_L and C_{My}. The experiments manifest a stronger lift coefficient and nose-up moment, except for angles of attack higher than 18° where breakdown starts to take place over the wing. By comparing the C_P distribution (Fig. 7) it is shown that the main strake vortex is already well predicted by the standard SAE model but the wing vortex is too strong compared to the wind tunnel measurements.

A new optimization procedure is prepared and performed considering two relevant angles of attack, namely 14° and 20°. The error is reduced and the improvement is consistent along the polar, except a slight discrepancy which remains at the highest angle of attack. From the C_P distribution (Fig. 7) it becomes evident that the effect of the turbulence model conditioning is concentrated in the second vortex which is misrepresented by the standard SAE model. The second vortex has a lower suction peak and it merges more rapidly into the main vortex which is only slightly influenced, accordingly with the experimental results. Overall the improvement is again good and promising but strictly related to the vortex topology which changes drastically with the fillet variation.

3.4 Conclusion and Outlook

The enhancement of the Salart-Allmaras one-equation eddy viscosity model for the numerical solution of vortex dominated flows is investigated and additional destruction terms are formulated. The terms influences are confirmed to be different accordingly with their formulation and this permits an improvement of the flexibility of the approach. The influence of the terms is confined to the vortex flow field and no numerical instability is introduced. An optimizer tool is implemented in order to calibrate the set of terms with experimental data as reference. The improvement of an optimized model variation is relevant, manifests low sensitivity on the angle of attack and small geometric variations. However, when the vortex topology is drastically altered by a more severe geometric or flow condition variation, the improvement becomes reduced and a new or a restart optimization may be required. For the considered test cases, the error between numerical solutions and experiments

for the angle-of-attack polar is reduced with the optimized turbulence model of 40% for the 65° swept delta wing and, for the 76°/40° double delta wing, of 44% with the baseline fillet and of 70% with the parabolic fillet. Therefore, for new test cases, values of error improvement in the range between 40% and 70% are expected. The globality of a traditional eddy viscosity model is therefore partially abandoned in favour of the accuracy enhancement. In order to extend the capability of the approach and define guidelines for the optimization and application procedure, the investigation of additional test cases or larger envelope of flow conditions are of high interest. Moreover, statistical information about the error improvement can be extrapolated when a relatively large amount of data is available.

4 Contact Author Email Address

For questions or information mailto:
matteo.moioli@aer.mw.tum.de

Acknowledgements

The support of this investigation by Airbus Defence and Space within the VitAM/VitaMInABC (Virtual Aircraft Model for the Industrial Assessment of Blended Wing Body Controllability, KFZ: 20A1504C) project is gratefully acknowledged. Furthermore, the authors thank the German Aerospace Center (DLR) for providing the DLR TAU-Code used for the numerical investigations and research. Moreover, the authors gratefully acknowledge the Gauss Centre for Supercomputing e.V. (www.gauss-centre.eu) for funding this project by providing computing time on the GCS Supercomputer SuperMUC at Leibniz Supercomputing Center (LRZ, www.lrz.de).

References

[1] Hummel D. *Experimental Investigation of the Flow on the Suction Side of a Thin Delta Wing*, NASA Technical Memorandum 75897, 1981.

[2] Lambourne N C and Dryer D W. Some Measurements in the Vortex Flow Generated by a Sharp Leading Edge Having 65 Degrees Sweep. *ARC Current Papers 477, Aeronautical Research Council*, 1960.

[3] Lambourne N C and Dryer D W. The Bursting of Leading-Edge Vortices. Some Observations and Disussions of the Phenomenon. *ARC Reports and Memoranda 3282, Aeronautical Research Council*, 1962.

[4] Wentz W H and Kohlman D L. Wind Tunnel Investigations of Vortex Breakdown on Slender Sharp-Edged Wings. *NASA Research Grant NGR-17-002-043, University of Kansas Center of Research, Inc., Engineering Sciences Division, Report FRL 68-013*, 1968.

[5] Fritz W and Cummings R M. What was learned from the numerical simulations for the VFE-2?. *AIAA Paper 2008-0399*, 2008.

[6] Schütte A, Hummel D and Hitzel S M. Flow Physics Analyses of a Generic Unmanned Combat Aerial Vehicle Configuration. *Journal of Aircraft*, Vol. 49, No. 6, pp 1638-1651, 2012.

[7] Crippa S and Rizzi A. Steady, Subsonic CFD Analysis of the VFE-2 Configuration and Comparison to Wind Tunnel Data. *AIAA Paper 2008-397*, 2008.

[8] Schütte A, Boelens O J, Oehlke M, Jirásek A and Loeser T. Prediction of the flow around the X-31 aircraft using three different CFD methods. *Aerospace Science and Technology*, Vo.20, No.1, pp 21-37, 2012.

[9] Cummings R M and Schütte A. Detached-eddy simulation of the vortical flow field about the VFE-2 delta wing. *Aerospace Science and Technology*, Vol. 24, No. 1, pp 66-76, 2013.

[10] Chu J and Luckring J M. Experimental Surface Pressure Data Obtained on 65° Delta Wing Across Reynolds Number and Mach Number Ranges. *NASA Technical Memorandum 4645, Langley Research Center*, Hampton, Virginia, 1996.

[11] Luckring J M and Hummel D. What was learned from the new VFE-2 experiments? *46th AIAA Aerospace Sciences Meeting and Exhibit*, Reno, Nevada, 2008.

[12] Erickson G E and Gonzalez H A. Wind Tunnel Application of a Pressure-Sensitive Paint Technique to a Double Delta Wing Model at Subsonic and Transonic Speeds. *NASA TM-2006-2143319, Langley Research Center*, Hampton,

Virginia, 2006.

[13] Spalart P R and Allmaras S R. A One-Equation Turbulence Model for Aerodynamic Flows. *30th AIAA Aerospace Sciences Meeting & Exhibit*, Reno, Nevada, 1992.

[14] Shur M L, Strelets M K, Travin A K and Spalart P R. Turbulence Modeling in Rotating and Curved Channels: Assessing the Spalart-Shur Correction. *AIAA Journal*, Vol. 38, No. 5, pp 784-792, 2000.

[15] Edwards J R and Chandra S. Comparison of Eddy Viscosity-Transport Turbulence Models for Three-Dimensional, Shock-Separated Flowfields. *AIAA Journal*, No. 4, pp 756-763, 1996.

[16] Truesdell C. The physical components of vectors and tensors. *ZAMM - Journal of Applied Mathematics and Mechanics / Zeitschrift für Angewandte Mathematik und Mechanik*, Vol. 33, No. 10-11, pp 345-356, 1953.

[17] Jeong J and Hussain F. On the identification of a vortex. *Journal of Fluid Mechanics, Cambridge University Press*, Vol. 285, pp 69-94, 1995.

[18] TAU-Code User Guide Release. *DLR Institute of Aerodynamics and Flow Technology*, 2015.

[19] Galle M, Evans J and Gerhold T. Technical Documentation of the DLR [Tau]-code. *DLR Institute of Aerodynamics and Flow Technology*, 1997.

Copyright Statement